

Online Journal of Space Communication

Volume 2
Issue 3 *Remote Sensing of Earth via Satellite*
(Winter 2003)

Article 15

January 2003

Multi-Sensor Image Registration, Fusion and Dimension Reduction

Jacqueline Le Moigne

Follow this and additional works at: <https://ohioopen.library.ohio.edu/spacejournal>



Part of the [Astrodynamics Commons](#), [Navigation, Guidance, Control and Dynamics Commons](#), [Space Vehicles Commons](#), [Systems and Communications Commons](#), and the [Systems Engineering and Multidisciplinary Design Optimization Commons](#)

Recommended Citation

Le Moigne, Jacqueline (2003) "Multi-Sensor Image Registration, Fusion and Dimension Reduction," *Online Journal of Space Communication*: Vol. 2 : Iss. 3 , Article 15.

Available at: <https://ohioopen.library.ohio.edu/spacejournal/vol2/iss3/15>

This Research Reports is brought to you for free and open access by the OHIO Open Library Journals at OHIO Open Library. It has been accepted for inclusion in Online Journal of Space Communication by an authorized editor of OHIO Open Library. For more information, please contact debord@ohio.edu.

Multi-Sensor Image Registration, Fusion and Dimension Reduction

Jacqueline Le Moigne

With the development of future spacecraft formations comes a number of complex challenges such as maintaining precise relative position and specified attitudes, as well as being able to communicate with each other. More generally, with the advent of spacecraft formations, issues related to performing on-board and automatic data computing and analysis as well as decision planning and scheduling will figure among the most important requirements. Among those, automatic image registration, image fusion and dimension reduction represent intelligent technologies that would reduce mission costs, would enable autonomous decisions to be taken on-board, and would make formation flying adaptive, self-reliant, and cooperative. For both on-board and on-the-ground applications, the particular need for dimension reduction is two-fold, first to reduce the communication bandwidth, second as a pre-processing to make computations feasible, simpler and faster.

At the same time, continuity of the data as well as extrapolation among several scales, temporal, spatial, and spectral, are key components of many remote sensing applications, and these properties are provided by integration and seamless mosaicking of multiple sensor data, via image registration and image fusion.

Image Registration

In this work, “image registration” is defined as a feature-based “precision correction,” in opposition to a model-based “systematic correction.” In our experiments, we assume that the data has already been systematically corrected according to a navigation model. The goal of a precision-correction algorithm is to utilize selected image features or control points to refine the geo-location accuracy given by the systematic model within one pixel or a sub-pixel. Currently, there is a large quantity of potential image registration methods that have been developed for aerial or medical images and that are applicable to remote sensing images [1,2]. But there is no consolidated approach to select the most appropriate method for a remote sensing application, given the type of data, the desired accuracy and the type of computational power available with respect to timing requirements. The intent of our work is to survey, design, and develop different components of the registration process and to evaluate their performance on well-chosen multi-sensor data.

As a general definition, automatic image registration of satellite image data is the process that aligns one image to a second image of the same scene that was acquired at the same or at different times by different or identical sensors. One set of data is taken as the *reference data*, and all other data, called *input data (or sensed data)*, is matched relative to the reference data. The general process of image registration includes three main steps:

- Extraction of features to be used in the matching process.
- Feature matching strategy and metrics.
- Data re-sampling based on the computed deformation (sometimes replaced by indexing or fusion).

Many choices are available for each of the previous steps [1,2]. Our work [3-12] has mainly been dealing with features such as gray levels, edges, and wavelet coefficients, and matching them using either cross-correlation, Mutual Information or a Hausdorff distance as a similarity metrics, and exhaustive search or optimization techniques as search strategies.

Our earlier work utilized cross-correlation as a similarity metrics to compare features such as gray levels, edges, and Daubechies wavelet coefficients using mono-sensor data [4]. Results showed that, as expected, edges or edge-like features like wavelets were more robust to noise, local intensity variations or time-of-the day conditions than original gray level values. At the same time, orthogonal wavelet-based registration was usually faster although not always as accurate than a full-resolution edge-based registration. This lack of consistent accuracy of orthogonal wavelets seemed to be due to their lack of translation-invariance. To study the effects of translation and rotation-invariance of wavelets, we conducted two studies:

(1) The first study [11] quantitatively assessed the use of orthogonal wavelet sub-bands as a function of features' sizes. The results showed that:

- Low-pass sub-bands are relatively insensitive to translation, provided that the features of interest have an extent at least twice the size of the wavelet filters (this result is in accordance with the Nyquist's criterion).
- High-pass sub-bands, although still useable for registration, are more sensitive to translation.

(2) The second study [6] investigated the use of an over complete frame representation, the "Steerable Pyramid" [13]. It was shown that, as expected and due to their translation- and rotation- invariance, Simoncelli's steerable filters performed better than Daubechies' filters. Rotation errors obtained with steerable filters were minimum, independent of rotation size. Noise studies also reinforced the results that steerable filters showed a better robustness to larger amounts of noise than orthogonal filters.

All previous work focused on correlation-based methods used with an exhaustive search. One of the main drawbacks of this method is the prohibitive computation times when the number of transformation parameters increases (e.g., affine transformation vs. shift-only), or when the size of the data increases (full size scenes vs. small portions, multi-band processing vs. mono-band). To answer some of these concerns, we investigated different types of similarity metrics and different types of feature matching strategies. In this study, five different algorithms were developed and compared. The features that were utilized were original gray levels and wavelet features. The different metrics were correlation, mutual information [14] and a Partial Hausdorff distance [15]. The strategies were exhaustive search, optimization and robust feature matching.

The multi-sensor dataset used for this study was acquired by four different sensors over one of the MODIS Validation Core Sites, the Konza Prairie in Kansas, United States, and included:

- IKONOS Bands 3 (Red) and 4 (Near-Infrared), spatial resolution of 4 meters per pixel.

- Landsat-7/ETM+ Bands 3 (Red) and 4 (Near-Infrared), spatial resolution of 30 meters per pixel.
- MODIS Bands 1 (Red) and 2 (Near Infrared), spatial resolution of 500 meters, per pixel.
- SeaWiFS Bands 6 (Red) and 8 (Near Infrared), spatial resolution of 1000 meters per pixel.

Compatible spatial resolutions were obtained by performing recursive decimation by 2 of the wavelet transform. Overall, all results obtained by the 5 algorithms were similar within 0.5 degrees in rotation and within 1 pixel in translation.

Then, subpixel registration capabilities of some of the previous algorithm components were assessed by registering a coarse image to a fine image at the resolution of the fine image. For this purpose, we utilized a multiphase filtering technique, in which all possible phases of the fine image are registered with respect to the coarse image. Each different phase is filtered and down-sampled to the coarse resolution. The phase that gives the best registration metric gives the registration to the resolution of the fine image. We registered this data using two different criteria, normalized correlation and mutual information. The results showed that both correlation and mutual information have an overall accuracy of about 0.5 pixels with a 0.25 pixel accuracy for same-band data.

Another way to look at the data is to analyze the self-consistency of the measurements. For this analysis, we considered 3 images and computed the (x,y) offset of one of the images from the other two in two different ways (i.e., [Image1 to Image 2] and [Image1 to Image3 to Image 2]). If the registrations are self-consistent, the answers should be the same. In this experiment, we showed that correlation and mutual information exhibited self-consistency within 1/8 pixel.

Image Fusion

After an accurate multi-sensor registration, the complementary information provided by different sensors with multiple spatial and spectral resolutions can be integrated through image fusion. This is the focus of the following investigation, characterization and mapping of land cover/land use of forest areas, such as the Central African rainforest. This task is very complex, mainly because of the extent of such areas and, as a consequence, because of the lack of full and continuous cloud-free coverage of those large regions by one single remote sensing instrument. In order to provide improved vegetation maps of Central Africa and to develop forest-monitoring techniques for applications at the local and regional scales, we are studying the possibility of utilizing multi-sensor remote sensing observations coupled with in-situ data. Fusion and clustering of multi-sensor data are the first steps towards the development of such a forest monitoring system. Our first experiments involve the fusion of SAR and Landsat image data of the Lopé Reserve in Gabon [18].

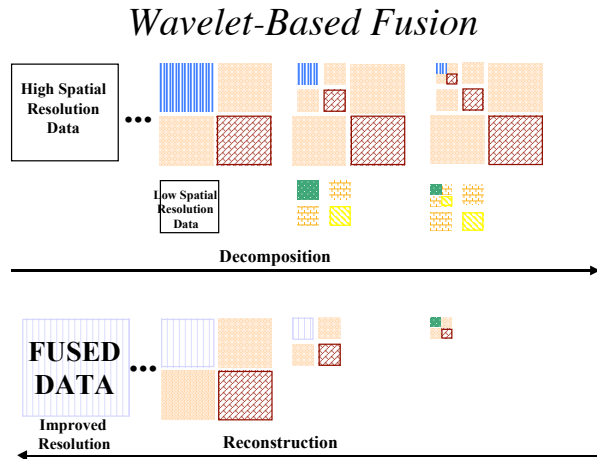


Figure 1 - Wavelet-Based Image Fusion

Similarly to previous fusion studies [16,17], our fusion method is wavelet-based. Figure 1 illustrates the wavelet-based fusion idea, where high- and low-resolution data are independently decomposed using a multi-resolution wavelet. Then, components from both decompositions are combined during the reconstruction phase to create the new fused data. In this scheme, low-frequency information of the lowest spatial resolution data (e.g., Landsat or MODIS data) are combined with high-frequency information of the highest resolution data (resp., SAR or JERS data) in order to take simultaneous advantage of the higher spatial and spectral resolutions. In this study, the same Daubechies filter size 4 was used for both decomposition and reconstruction phases and for both types of data. But we are now investigating the use of different filters for decomposition and reconstruction as well as for high- and low-resolution data that would better preserve the spatial, spectral and textural properties of the data. The fusion stage is followed by unsupervised classification, first to validate our fusion method, and then to obtain a vegetation map of the area of interest. The classification obtained after fusion of SAR and Landsat is then compared to the classification obtained from Landsat data alone. Results are shown in Figures 2 and 3, where dark green, light green, orange, light blue, pink, and dark blue represent respectively Mountain Forest, Mixed Forest, Okoume Forest, Savanna, Fern Savanna, and Burnt Savanna. Qualitatively, we can see that the results are similar, but that the fused clustering shows more localized details with differentiation of the different types of savannas in the right side of the image and a different clustering of Mountain Forest versus Mixed Forest in the left side of the image. These results will be evaluated quantitatively, once in-situ data become available.

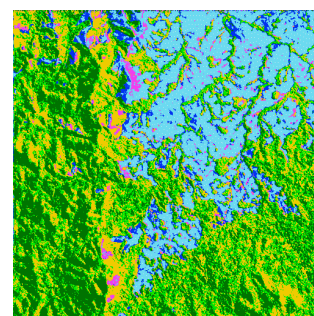
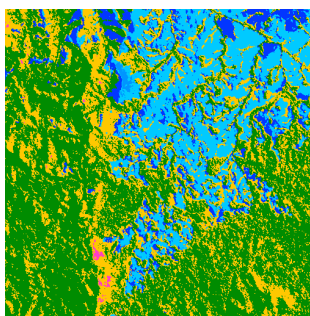


Figure 2 - Landsat Classification**Figure3 - Fused Data Classification*****Dimension Reduction***

The introduction of hyperspectral instruments results in a large increase of remote sensing data volumes. Dimension reduction of such data, by filtering out redundant information, can reduce data volumes and speed up further processing, such as supervised or unsupervised classification. Considering such data increases, and anticipating the ultraspectral instruments of the future, we investigated existing methods such as the Principal Component Analysis (PCA) and its implementation on a parallel architecture like the COTS-based Beowulf architecture. We also looked at a parallel adaptive PCA [19], and we developed a new wavelet-based dimension reduction method [20].

Adaptive and Parallel Principal Component Analysis

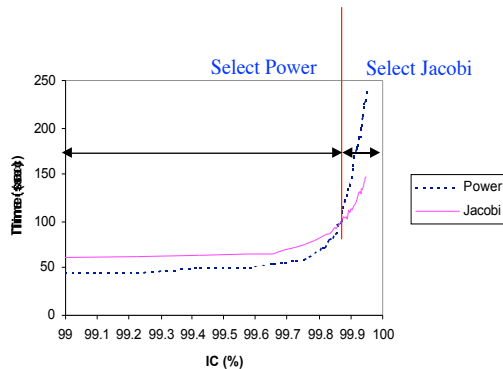
Due to its conceptual simplicity, Principal Component Analysis (PCA) is the most widely used among dimension reduction techniques. The general idea of this process is to project the data in a different coordinate system and to obtain a lower dimension that provides a compact and uncorrelated representation of the data. The first principal component (PC1) has the largest percentage of the overall data variance, also representing the "information content." The following principal components, from component number 2 to n, contain a decreasing percentage of total data variation.

Because of the high computational demands of PCA, its implementation on a parallel processor needs to be addressed. Two basic methods for performing the PCA computations are considered: the power method and the Jacobi method. The power method computes the eigenvalues one by one starting with the largest one (which is associated with the PC that contains most of the information), then moving to the next largest and so on. The power method, therefore, offers the opportunity to only compute the eigenvalues and the PCs that correspond to a desired level of information content. The Jacobi method computes all eigenvalues at once, and therefore may require a higher execution time. But, in a parallel implementation, the Jacobi method scales better than the power method when a larger number of the PCs are computed. Thus, for cases where a relatively small level of information content is needed, the power method could work faster, while, when a higher level of information content is needed, the Jacobi method should be used instead.

As a consequence, we developed an adaptive algorithm that quickly reduces the dimensionality of hyperspectral data by adaptively selecting which of the two methods to use, depending on the number of PC's needed or equivalently depending on the desired level of information content. Experimental results not only show scalability, but also demonstrate that the execution time of this application has been brought to feasible levels using a cost-efficient high performance computer, a Pentium-based Beowulf System. Both algorithms and the adaptive method were tested on hyperspectral data obtained from the AVIRIS imaging spectrometer, with a spatial resolution of 17m x 17m and a spectral resolution of 224 channels. As a parallel architecture, we used a Beowulf machine

developed at NASA/Goddard, the HIVE (Highly-parallel Integrated Virtual Environment), which consists of four sub-clusters containing a total of 332 processors. In this work, we use a sub-cluster with 2 dual-Pentium Pro host nodes, and 66 dual-Pentium Pro PCs (132 processors) working as compute nodes.

As an illustration, Figure 4 shows the timing and specific crossing point (in terms of information content) at which one or the other of the algorithms, Jacobi or Power, needs to be selected.



Time and Information Content

PCs	IC (%)	Power-based	Jacobi-based
20	99.85127	87.08 sec	92.05 sec
21	99.85638	96.74 sec	94.71 sec

Figure 4 - Timing and Switching Decision for the AVIRIS Data (Sequential Implementation)

In implementing the parallel algorithms, special attention was given to the fact that communication bandwidth and latency in clusters do not compare favorably with processing speed. For example, computing the mean in the master node and broadcasting it is more efficient than computing the mean in parallel. Table 1 shows the execution time for 2, 4, 8, and 16 processors. For the same underlying hardware, the specific crossing point differs based on the data set. The general implication for the adaptive algorithm is that a threshold of 99 percent information content can be used, and will ensure that the adaptive algorithm is performing at or around the optimal execution time for computing the desired PCs.

PEs	PCs	IC (%)	Parallel Time Power-Based	Parallel Time Jacobi-Based
2	3	99.11751	4.482	4.526
	4	99.40379	5.509	4.676
4	18	99.88254	5.303	5.313
	19	99.88767	5.651	5.466
8	22	99.90222	3.645	3.693
	23	99.90674	3.888	3.783
16	23	99.90674	3.859	3.978
	24	99.91116	4.738	3.79

Table 1 – Execution Time on the Hive; PEs = Number of Processors; PCs = Number of Principal Components; IC = Information Content (in percent)

A Wavelet-Based Dimension Reduction Technique

The principle of this wavelet-based method is to apply a discrete one-dimensional wavelet transform to hyperspectral data in the spectral domain and at each pixel. Figure 5 shows an example of the actual signature of one class (Corn-notill) for 192 bands of an AVIRIS dataset, and different levels of wavelet decomposition of this spectral signature. When the number of bands is reduced, the structure of the spectral signature becomes smoother than the structure of the original signature, but the signal still shows the most important features for several levels. Once the 1-D wavelet decomposition is applied to each pixel signature, the wavelet coefficients yield a reduced-dimensional data set that can be used for applications such as supervised classification.

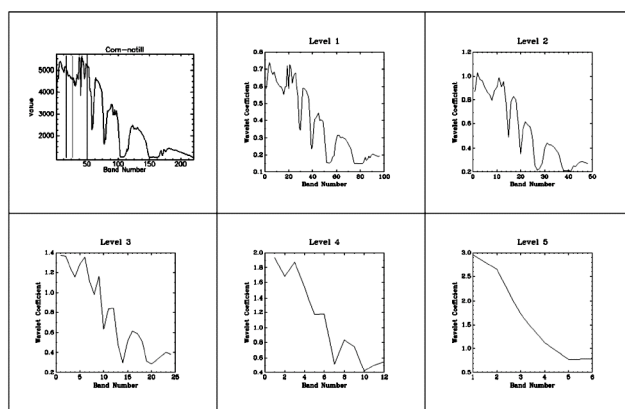


Figure 5 - An example of the Corn-notill spectral signature and different levels of wavelet decomposition

From a complexity point of a view, the wavelet-based reduction method yields the order of $O(MN)$, where N is the number of bands and M is the number of pixels in the spatial domain. On the other hand, the total estimated complexity of PCA is $O(MN^2+N^3)$, which shows that the computation efficiency of a wavelet reduction technique is superior to the efficiency of the PCA method.

Validation of the wavelet-based reduction is performed using supervised classification with 1992 AVIRIS data of the northern part of Indiana (US). The results (Table 2) show that our new wavelet-based reduction technique provides a greater computational efficiency as well as a better overall classification accuracy than the widely used PCA method. For this dataset and the Maximum Likelihood (ML) classification, it is shown that the Wavelet Reduction gives 79% overall accuracy for the third level of decomposition, while PCA only gives 77.5% for an equivalent 24 PCs for the ML classification or 81% versus 79% for an equivalent 48PC's. The same trend was seen with another AVIRIS dataset. The two other classification methods, Minimum Distance and Parallelepiped, used for comparison purpose, are sometimes chosen over the Maximum Likelihood classification because of their speed, but are known to be much less accurate than the ML classification.

Classification Method	Reduction Method	Classification Accuracy (%)			
		No. of Component/Level of Decomposition			
		48/2	24/3	12/4	6/5
<i>Maximum Likelihood</i>	<i>Wavelet</i>	80.9647	78.9956	73.3476	66.8142
	<i>PCA</i>	79.0057	77.4945	73.546	70.6915
<i>Minimum Distance</i>	<i>Wavelet</i>	50.5979	50.4554	49.8601	48.6796
	<i>PCA</i>	50.6335	50.608	50.6182	50.5012
<i>Parallelepiped</i>	<i>Wavelet</i>	33.7658	33.7862	32.4174	31.1759
	<i>PCA</i>	28.4181	28.8964	28.4181	28.3824

Table 2

Different types of classifications of PCA vs. wavelet, different levels of decomposition (IndianPines'92)

In summary, both analytical assessment of time complexity and experimental results of classification accuracy have proven that the 1-D wavelet-based dimension reduction technique is an efficient method in reducing dimensionality of hyperspectral data. Its performance, assessed through classification accuracy, is comparable and often superior to the PCA method performance.

References

1. A. Goshtasby, J. Le Moigne, "Special Issue Image Registration," *Pattern Recognition*, V.32, N.1, 1999.
2. L. Brown, "A Survey of Image Registration Techniques," *ACM Computing Surveys*, vol. 24, no.4, 1992.
3. J. Le Moigne, W.J. Campbell, and R.F. Crompt, "An Automated Parallel Image Registration Technique of Multiple Source Remote Sensing Data," *IEEE Transactions on Geoscience and Remote Sensing*, Vol. 40, No. 8, pp. 1849-1864, August 2002.
4. J. Le Moigne, W. Xia, J. Tilton, T. El-Ghazawi, M. Mareboyana, N. Netanyahu, W. Campbell, R. Crompt, "First Evaluation of Automatic Image Registration Methods," *IGARSS'98*, July 1998
5. J. Le Moigne, "Parallel Registration of Multi-Sensor Remotely Sensed Imagery Using Wavelet Coefficients," *SPIE Aerospace Sensing, Wavelet Applications*, Orlando, 1994.
6. J. Le Moigne, and I. Zavorin, "Use of Wavelets for Image Registration," *SPIE Aerosense 2000, "Wavelet Applications VI"*, Orlando, FL, April 24-28, 2000.
7. D. Mount, N. Netanyahu, J. Le Moigne, "Efficient Algorithms for Robust Feature Matching," *Pattern Recognition on Image Registration*, Vol. 32, No. 1, January 1999.
8. J. Le Moigne, N. Netanyahu, J. Masek, D. Mount, S. Goward, "Robust Matching of Wavelet Features for Sub-Pixel Registration of Landsat Data," *IGARSS'01*, Sydney, Australia, July 9-13, 2001
9. J. Le Moigne, A. Cole-Rhodes, R. Eastman, K. Johnson, J. Morissette, N. Netanyahu, H. Stone, and I. Zavorin, "Multi-Sensor Registration of Earth Remotely Sensed Imagery," *8-th SPIE Int. Symp. Remote Sensing, Image and*

- Signal Processing for Remote Sensing VII*, Vol. #4541, France, September 2001.
10. R. Eastman and J. Le Moigne, "Gradient-Descent Techniques for Multi-Temporal and Multi-Sensor Image Registration of Remotely Sensed Imagery," *FUSION'2001, 4-th International Conference on Information Fusion*, Montreal, Canada, August 7-10, 2001.
 11. H. Stone, J. Le Moigne, and M. McGuire, "Image Registration Using Wavelet Techniques," *IEEE-PAMI*, 21, 10, 1999.
 12. K. Johnson, A. Rhodes, J. Le Moigne I. Zavorin, "Multi-resolution Image Registration of Remotely Sensed Imagery using Mutual Information," *SPIE Aerosense "Wavelet Applications VII"*, April 2001.
 13. E. Simoncelli, W. Freeman, "The Steerable Pyramid: A Flexible Architecture for Multi-Scale Derivative Computation," *2-nd IEEE ICIP*, 1995.
 14. F. Maes, A. Collignon, D. Vandermeulen, G. Marchal, P. Suetens, "Multimodality Image Registration by Maximization of Mutual Information," *IEEE Trans. on Medical Imaging*, Vol. 16, No.2, April 1997.
 15. D.P. Huttenlocher, G.A. Klanderman, and W.J. Rucklidge, "Comparing Images Using the Hausdorff Distance," *IEEE Transactions on Pattern Analysis Machine Intelligence*, Vol. 15, 1993, pp. 850--863.
 16. C. Pohl, and J.L. Van Genderen, "Multisensor Image Fusion in Remote Sensing: Concepts, Methods and Applications," *International Journal of Remote Sensing*, vol. 19, No. 5, pps. 823-854, 1998.
 17. T. Ranchin, and L. Wald, "Data Fusion of Remotely Sensed Images Using the Wavelet Transform: the ARSIS Solution," *Proceedings SPIE Wavelet Applications in Signal and Image Processing IV*, 1997.
 18. J. Le Moigne, N. Netanyahu, and N. Laporte, "Enhancement of Tropical Land Cover Mapping with Wavelet-Based Fusion and Unsupervised Clustering of SAR and Landsat Image Data," *Proceedings of the 8-th SPIE International Symposium on Remote Sensing, Image and Signal Processing for Remote Sensing VII*, Vol. #4541, Toulouse, France, September 17-21, 2001.
 19. T. El-Ghazawi, S. Kaewpjit, J. Le Moigne, "Parallel and Adaptive Reduction of Hyperspectral Data to Intrinsic Dimensionality," *CLUSTER'01, IEEE Intern. Conf. on Cluster Computing*, CA., Oct. 2001.
 20. S. Kaewpjit, J. Le Moigne, and T. El-Ghazawi. "Spectral Data Reduction via Wavelet Decomposition," *Proc. of SPIE, Wavelet Applications IX*, 4-5 April 2002, Orlando, Florida.